

## Basic Science and Experimental Studies

# FN14 Signaling Plays a Pathogenic Role in a Mouse Model of Experimental Autoimmune Myocarditis

ANDREA FISCHER,<sup>1</sup> MARIELLA BOCKSTAHLER, PhD,<sup>1,2</sup> ANNA-MARIA MÜLLER, PhD,<sup>1,3</sup> VERA STROIKOVA,<sup>1</sup> CHRISTOPH LEIB, MD, PhD,<sup>1,2</sup> GABRIELE PFITZER, MD,<sup>3</sup> HUGO A. KATUS, MD,<sup>1,4</sup> AND ZIYA KAYA, MD<sup>1,4</sup>

Heidelberg, and Cologne, Germany; and Basel, Switzerland

## ABSTRACT

**Background:** The pathogenesis of inflammatory cardiomyopathy is affected by the activation of autoimmune-mediated cascades. To study these cascades, we developed an experimental model of troponin I (TnI)-induced autoimmune myocarditis (EAM). One factor playing a pivotal role in the context of autoimmune disorders is the receptor fibroblast growth factor-inducible 14 (FN14). Thus, the impact of FN14 in the development of autoimmune myocarditis was investigated.

**Methods and Results:** TnI-immunization led to a significantly increased myocardial FN14 mRNA and protein expression in wild-type (wt) mice. To investigate the precise role of FN14 in EAM, FN14 knockout (ko) and wt littermates were immunized with TnI or control buffer. The animals were evaluated for cardiac parameters and indicators of myocardial injury. FN14 deficiency resulted in better cardiac performance, less myocardial inflammation, fibrosis, and cardiac damage. A lower myocardial mRNA expression of inflammatory cytokines and chemokines as well as their receptors could be demonstrated in TnI-immunized FN14ko compared to wt mice also immunized with TnI. Western blot analysis revealed a contribution of nuclear factor kappa-light-chain-enhancer of activated B cells to FN14-induced signaling cascades.

**Conclusions:** In the pathogenesis of autoimmune myocarditis, the inflammatory response to cardiac injury is attenuated in FN14ko mice. Thus, inhibition of FN14 in patients might represent a novel therapeutic strategy in the treatment of inflammatory cardiomyopathy. (*J Cardiac Fail* 2019;25:674–685)

**Key Words:** Inflammation, cytokines, heart failure, Nfkb.

## Introduction

With ~17.3 million of deaths per year, cardiovascular diseases are still a leading cause of death worldwide.<sup>1</sup> In patients younger than 40, who suffer from cardiovascular diseases, myocarditis is the main reason for heart failure.<sup>2</sup>

A myocarditis can be induced by viral or bacterial infection, medication, radiation, ischemic events, or autoimmune reactions.<sup>3</sup> Cardiac damage, mediated by these factors, may result in the presentation of endogenous antigens to the immune system, which could cause an autoimmune response against cardiac tissue. Such an autoimmune response could lead to a perpetuation of immune-mediated cardiac damage involving either cellular (eg, T and B lymphocytes, dendritic cells), and/or humoral (eg, antibodies, cytokines) autoimmune responses. This immune-mediated cardiac damage finally results in an inflammation of the myocardium with concomitant impairment of cardiac function. Despite intensive research within the field of inflammatory cardiomyopathies, the molecular and cellular pathomechanisms leading to myocardial inflammation and cardiac dysfunction are not fully understood. To study principle pathomechanisms of autoimmune-based cardiomyopathies, our group developed a mouse model of troponin I (TnI)-induced experimental autoimmune myocarditis (EAM) mimicking the chronic phase of the human myocarditis. Here, immunization of mice with TnI induces severe

From the <sup>1</sup>Department of Medicine III, University of Heidelberg, 69120 Heidelberg, Germany; <sup>2</sup>Cardiology, St. Claraspital, 4058 Basel, Switzerland; <sup>3</sup>Institute of Vegetative Physiology, University of Cologne, 50931 Cologne, Germany and <sup>4</sup>DZHK (German Centre for Cardiovascular Research), partner site Heidelberg/Mannheim, University of Heidelberg, 69120 Heidelberg, Germany.

Manuscript received November 15, 2018; revised manuscript received May 26, 2019; revised manuscript accepted June 11, 2019.

Reprint requests: Ziya Kaya, Department of Cardiology, University of Heidelberg, Im Neuenheimer Feld 410, 69120 Heidelberg, Germany. Tel.: +49 6221 5639617; Fax: +49 6221 565516. E-mail: [ziya.kaya@med.uni-heidelberg.de](mailto:ziya.kaya@med.uni-heidelberg.de)

Funding: This research did not receive any specific grant from funding agencies in the public, commercial, or not-for-profit sectors.

See page 683 for disclosure information.

1071-9164/\$ - see front matter

Published by Elsevier Inc.

<https://doi.org/10.1016/j.cardfail.2019.06.003>

inflammation, fibrosis, impaired left ventricular ejection fraction (LVEF) and an increased myocardial damage.<sup>4</sup>

One important mediator of autoimmune reactions is the receptor fibroblast growth factor-inducible 14 (FN14). FN14 is a type I transmembrane protein belonging to the tumor necrosis factor (TNF) receptor superfamily. Activation of FN14 signaling cascades by Tumor necrosis factor-like weak inducer of apoptosis (TWEAK), the only ligand of FN14, affects cell proliferation and differentiation, apoptosis, angiogenesis as well as induction of inflammatory cytokines.<sup>5,6</sup> FN14 is expressed in almost all cell and tissue types, including cardiomyocytes.<sup>7,8</sup> Primary T and B lymphocytes are the only FN14-negative cells described so far.<sup>7</sup>

The clinical relevance of FN14 signaling could be already demonstrated in different autoimmune disorders like systemic lupus erythematosus and rheumatoid arthritis.<sup>9–13</sup> Moreover, the role of FN14 signaling was investigated in different animal models of inflammatory diseases.<sup>9</sup> Here, FN14 knockout (ko) mice showed a better outcome in a lupus and colitis model.<sup>14,15</sup> Nevertheless, FN14 signaling not only plays a role in the immune but also in the cardiovascular system.<sup>16–18</sup> A role of FN14 in the pathogenesis of autoimmune heart diseases is rather likely. Accordingly, we investigated the FN14 signaling in the model of TnI-induced EAM to better understand its contribution to the induction and progression of autoimmune myocarditis.

## Methods

### Experimental Autoimmune Myocarditis

For all experiments 5- to 6-week-old female A/J mice were used. A/J wild-type (wt) mice were obtained from Envigo (Huntingdon, Cambridgeshire, PE28 4HS, United Kingdom). FN14ko mice were kindly provided by Biogen and backcrossed to A/J background for at least 6 generations.<sup>19</sup> All mice were maintained in the animal facility unit of the University of Heidelberg, Germany. The Animal Care and Use Committee of the University of Heidelberg approved all procedures involving the use and care of animals (German animal protection code, G-100/13). Experiments were conducted according to the guidelines formulated by the European Community for experimental animal use (Directive 2010/63/EU).

To induce an EAM, A/J wt or FN14ko mice were immunized 3 times with 120  $\mu$ g murine cardiac TnI in supplemented complete Freund's adjuvant (CFA) with 5 mg/mL of *Mycobacterium tuberculosis H37Ra* (Sigma-Aldrich, St Louis, MO) and sacrificed on day 21. As a control group, mice were immunized with control-buffer (CFA+PBS) alone.

### Echocardiography

Echocardiographic measurements were performed using VisualSonics Vevo 2100 system, 30 MHz linear MicroScan transducer (MSH400), specially optimized for cardiovascular experiments in mice. Parasternal long-axis projection cine loops were acquired at the level of clear visible walls of the

aortic annulus. LVEF and stroke volume were determined by appropriate software, provided with the Vevo2100 platform. M-mode of the short axis was used to determine LV mass and interventricular septum thickness (IVS).

### Determination of High-Sensitive Troponin T

Serum samples were collected on day 21 when the mice were sacrificed. To determine the severity of myocardial damage, the high-sensitive troponin T (hs-TnT) level was measured by electrochemiluminescence (Elecsys 2010 analyzer, Roche Diagnostics, Germany). Serum samples were diluted (1:20) with 0.9% NaCl solution. Details of the test principle have been described before.<sup>20</sup>

### Histopathology and Immunohistochemistry

Mice were sacrificed under anesthesia with ketamine–xylazine (120 mg/kg:16 mg/kg intraperitoneal) by cervical dislocation. Hearts were removed and cut longitudinal vertical to septum into 2 pieces.

Half of a heart was fixed in 10% formalin and subsequently embedded in paraffin. The remaining part of the heart was snap-frozen in nitrogen for further investigations. Sections of 3–5  $\mu$ m thickness were cut and stained with hematoxylin and eosin (HE) to determine the level of inflammation. Five sections of each heart were inspected in a double-blinded manner by 2 independent investigators under light microscopy to evaluate inflammation. Here, the area infiltrated by immune cells was considered in relation to the whole heart section. The ratio (inflamed area of the section/ whole section) was specified in percentage. The mean infiltration (in percentage) was calculated from the values determined by the 2 investigators. Additionally, Masson's trichrome or Acid Fuchsin Orange G (Afog) staining was performed to detect collagen deposition to assess the grade of fibrosis. For specific quantification of fibrosis, the amount of the blue-stained collagen was quantified using the MRI fibrosis tool in combination with the color deconvolution tool of the image software Fiji and calculated as percentage of the whole heart section.

For immunohistochemical detection of infiltrated T lymphocytes (CD4, CD8), B lymphocytes (CD45), and macrophages (CD68) serial sections of 0.5  $\mu$ m thickness were cut. After heat-induced epitope retrieval for 30 minutes, sections were incubated with primary antibody (Supplementary Table S1) overnight at 4 °C (CD8, CD45, CD68). Subsequently, the sections were washed and incubated with secondary antibody (horseradish peroxidase-coupled anti-rat IgG, 1:500) for 25 minutes followed by incubation with streptavidin horseradish peroxidase complex for 25 minutes. Antigens were visualized using Dako REAL Detection System. The detection of CD4-positive cells was performed using the SuperVision2Red-single Species rabbit AP kit according to the manufacturer's instructions. The incubation with primary antibody was carried out for 1 hour at room temperature. For quantifying infiltrated leukocytes, 4 high-power fields (40x magnification) were counted per slide and the number of positive cells was calculated per mm<sup>2</sup>.

### Quantitative Real-Time Polymerase Chain Reaction

RNeasy Fibrous Tissue Mini Kit (Qiagen, Hilden, Germany) was used according to the manufacturer's instructions to isolate total RNA from snap-frozen heart tissue. An amount of 1  $\mu$ g RNA was used for cDNA synthesis (iScript gDNA Clear cDNA Synthesis Kit, Bio-Rad, Munich, Germany). The quantification was done by using iTaq universal SYBR Green supermix (Bio-Rad) according to the manufacturer's instructions and using an iCycler iQ2 Detection System (Bio-Rad). An amount of 50 ng of cDNA in a 10  $\mu$ L reaction volume was used. A denaturation step at 95 °C for 5 minutes was carried out, followed by 40 cycles of denaturation at 95 °C for 10 seconds and annealing at 60 °C for 30 seconds. Primer sequences are listed in Supplementary Table S2. The measured gene expressions were normalized to the expression of the reference gene L32 as well as to the expression of the analyzed genes in control immunized mice by the application of following formula:  $r = 2^{-\Delta\Delta CT}$ .

Indicated relative expression is the mean of 3 independent technical replicates.

### Western Blotting

For Western blot analysis, snap-frozen heart tissue was ground in lysis buffer (50 mM Tris/HCl, 250 mM NaCl, 0.1% Triton X-100, 5 mM EDTA, 50 mM NaF) completed with 0.1 mM DTT and Halt™ Protease and Phosphatase Inhibitor Cocktail (Life Technologies, Darmstadt, Germany) and incubated on ice for 30 minutes. Samples were centrifuged at 18,000 g for 20 minutes. The supernatant was used to determine protein concentrations using Protein Assay Bradford reagent (Bio-Rad).

Ten micrograms of total myocardial protein extract per lane were separated on NuPAGE Bis-Tris gels (Invitrogen, Darmstadt, Germany) and transferred to a polyvinylidene fluoride transfer membrane (Millipore Immobilon-P; Millipore, Schwalbach, Germany). The membrane was first blocked with 5% nonfat dry milk in 0.1% TBST for 1 hour at room temperature and then incubated with primary antibody (Supplementary Table S1) overnight at 4 °C. After several washing steps, the blots were incubated with secondary antibody (horseradish peroxidase-coupled anti-rabbit IgG, 1:10,000, horseradish peroxidase-coupled anti-goat IgG, 1:10,000) for 1 hour at room temperature. Protein bands were detected using a chemiluminescence agent (GE Healthcare, Buckinghamshire, UK). Quantitative analysis was performed with FluorChem Q software. GAPDH served as a loading control. Indicated relative expression is the mean of 3 independent technical replicates.

### Statistical Analysis

Results are expressed as mean  $\pm$  SEM. For the comparison of 2 groups, the groups were tested for normal distribution with the D'Agostino–Pearson test. Differences between 2 parametric groups were tested with unpaired *t* tests. For 2 nonparametric groups, Mann–Whitney test was used. For the comparison of >2 groups, two-way ANOVA with

conservative Bonferroni post hoc test was used to control the type I error rate. As independent variables the genotype (wt vs FN14ko) and the treatment (control vs TnI) were tested. Values of  $P < 0.05$  were considered statistically significant and marked by \* $P < 0.05$ , \*\* $P < 0.01$ , \*\*\* $P < 0.001$ . Analysis was performed with GraphPad Prism 7.

## Results

### TnI-Immunization Increases Myocardial mRNA and Protein Levels of FN14

After TnI and control immunization in wt mice, expression of myocardial FN14 mRNA level was determined by quantitative real-time polymerase chain reaction (qPCR). TnI-immunized mice showed a significantly increased FN14 mRNA expression level compared to the control group 21 days after the first immunization (Fig. 1A). Furthermore, Western blot analysis also revealed a significantly increased FN14 protein expression 21 days after EAM induction (Fig. 1B, C).

### FN14 Deficiency Resulted in Less Myocardial Inflammation and Fibrosis, Cardiac Damage, and Cardiac Performance Compared to wt

Because of immunization-dependent alterations in FN14 expression, the role of FN14 in EAM was further investigated. Therefore, FN14ko mice as well as wt mice were immunized with TnI or control and different parameters for the evaluation of disease outcome were determined. FN14ko mice showed significantly less inflammation and fibrosis within the myocardium after TnI-immunization (Fig. 2A, B). Furthermore, TnI-immunized FN14ko mice displayed significantly lower hs-TnT levels than the wt group (Fig. 2C). A significantly lower heart weight to body weight ratio could be detected in TnI-immunized FN14ko mice compared to wt mice (Fig. 2D). Additionally, 21 days after starting with EAM-induction, transthoracic echocardiography showed an improved cardiac performance in FN14ko mice compared to their wt littermates. This improved cardiac performance was expressed by a significant better LVEF of FN14ko mice compared to wt mice on day 21. Apart from that, TnI-immunized FN14ko mice showed a significantly higher stroke volume compared to wt mice. LV Mass was significantly lower in ko compared to wt mice after TnI-immunization. TnI-immunized wt mice displayed increased interventricular septum thickness (IVS) compared to FN14ko mice (Fig. 2E; Supplementary Table S3).

No further differences could be detected for any of the investigated parameters between control-immunized wt and ko mice (Fig. 2A–E).

### FN14 Has an Impact on Infiltrating Immune Cells of the Innate As Well As the Adaptive Immune Response

To investigate whether the milder progression of EAM in FN14ko mice is based on specific cell types, the infiltrated leukocytes in the myocardium were immunohistochemical differentiated in CD4 and CD8 T lymphocytes, B

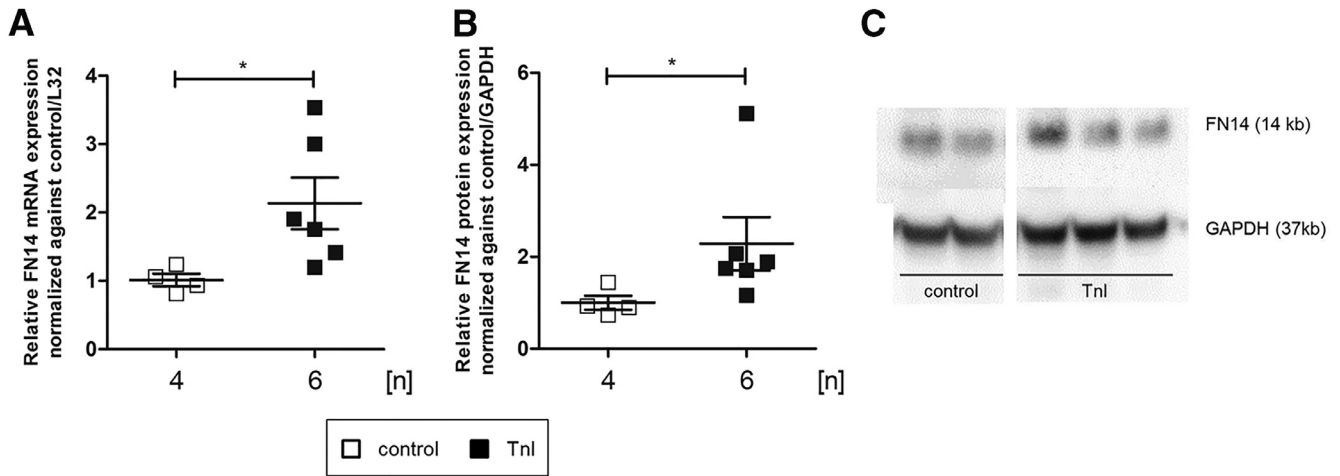


**Fig. 1.** Altered expression of FN14 in EAM model. Female A/J mice were immunized with TnI (n = 6) or control (n = 4) and sacrificed on day 21. Relative mRNA expression of FN14 (control:  $1.01 \pm 0.09$  vs TnI:  $2.13 \pm 0.38$ ;  $P < 0.05$ ) was determined (A). Western blot analysis for FN14 protein expression (control:  $1.00 \pm 0.15$  vs TnI:  $2.283 \pm 0.581$ ;  $P < 0.05$ ) was performed (B). Representative Western blot images for detection of FN14 protein expression. Ten micrograms of protein were used for detection of FN14 protein expression. GAPDH served as loading control (C). Data are depicted as mean ± SEM. Statistical analysis was performed using Mann–Whitney  $U$  test.

lymphocytes, as well as macrophages. Here, a significantly lower infiltration of CD4 T lymphocytes, B lymphocytes, and macrophages could be detected in TnI-immunized FN14ko mice compared to wt mice. The infiltration with CD8 T lymphocytes could be observed to a very low number for both wt and ko mice. Here, no difference could be detected dependent on the genotype (Fig. 3).

### Myocardial mRNA Expression Levels Display Anti-Inflammatory Phenotype in FN14ko Mice

To evaluate the contribution of the immune system to the significantly reduced inflammation and fibrosis in FN14ko mice, mRNA expression of chemokines and their receptors was determined between FN14ko and wt mice. The myocardial mRNA expressions of monocyte chemoattractant protein (MCP) 1, C–C chemokine receptor type (CCR) 1, CCR2, and CCR5 were significantly lower in TnI-immunized FN14ko mice compared to wt littermates. No significant expression changes of macrophage inflammatory protein (MIP1)  $\alpha$  and MIP1 $\beta$  could be detected between TnI-immunized and control-buffer-immunized ko mice, whereas wt mice showed significant changes in expression of these 2 genes after EAM-induction. Expression of regulated on activation, normal T cell expressed and secreted (RANTES) was increased during EAM in both ko and wt mice (Fig. 4A, B). Furthermore, the myocardial mRNA expression of the inflammatory cytokines like TNF $\alpha$ , interleukin (IL) 6, and IL17 showed significantly decreased levels in TnI-immunized ko compared to wt mice. Expression of IL1 $\beta$  was decreased in FN14ko compared to wt mice after EAM induction by tendency. Here, a significant increase of IL1 $\beta$  mRNA expression could be observed in TnI-immunized wt mice compared to control group, whereas FN14ko mice showed no difference depending on immunization (Fig. 4C). Matrix metalloproteinase (MMP)

expression level revealed for MMP9 a difference in wt between control-buffer and TnI and for MMP14 between TnI-immunized wt and FN14ko mice. No differences could be detected for MMP2 neither between control-buffer and TnI nor between wt and ko mice (Fig. 5).

The highest increases in mRNA expression of the investigated genes arise from the same mice.

### FN14 Signaling Activated Nuclear Factor Kappa-Light-Chain-Enhancer of Activated B-Cell Pathway

Analysis of nuclear factor of kappa light polypeptide gene enhancer in B-cell inhibitor, alpha ( $I\kappa B\alpha$ ) protein expression revealed that TnI-immunization led to a decreased  $I\kappa B\alpha$  protein expression in wt, but not FN14ko-mice (Fig. 6A, B). Furthermore, protein expression of the p50 precursor protein p105 was slightly increased in TnI-immunized wt- compared to FN14ko-mice. Protein expression of p50 was significantly higher in TnI-immunized wt- compared to FN14ko-mice (Fig. 6C–E).

### Discussion

Inflammatory cardiomyopathy is a leading cause of dilated cardiomyopathy, which in turn is considered to be one of the most common reasons for heart failure.<sup>21,22</sup> The molecular pathomechanisms involved in the induction of an inflammatory cardiomyopathy have not been completely understood so far. This lack of knowledge can be referred to various endogenous and exogenous agents mediating autoimmune reactions including both cellular and humoral response.<sup>21</sup> One important mediator of autoimmune reactions in general is the FN14 receptor, which supports cellular and humoral response via the activation of nuclear factor kappa-light-chain-enhancer of activated B cells (NF $\kappa$ B).<sup>7</sup> Thus, the contribution of FN14 to autoimmune reactions suggests the assumption that FN14 could also play a pivotal role in the pathogenesis of an EAM.

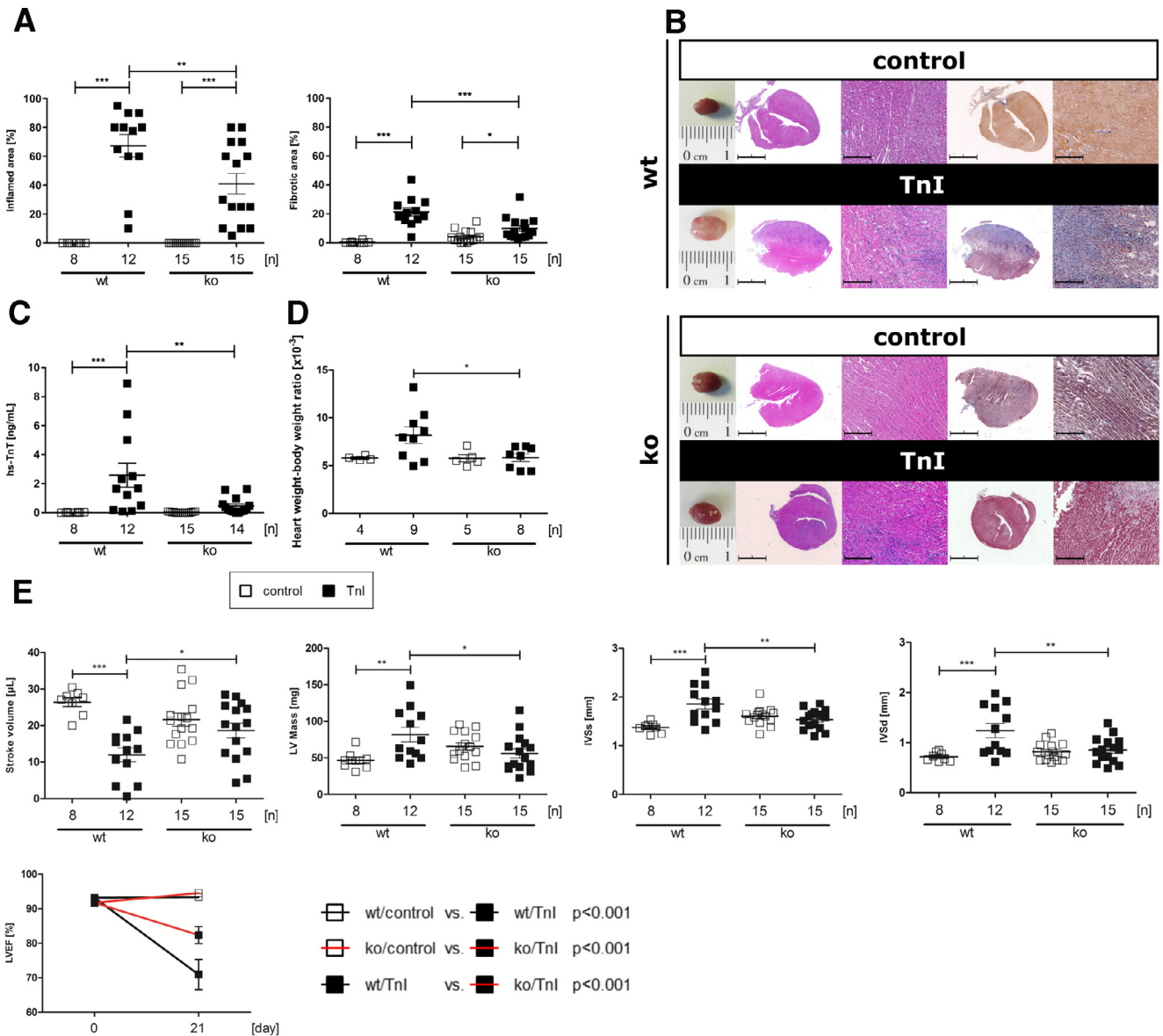


**Fig. 2.** FN14ko mice showed reduced inflammation and preserved function in TnI-induced EAM. FN14ko mice and wt littermates were immunized with TnI or control and sacrificed on day 21. Histocore of cardiac inflammation and fibrosis of immunized mice were significantly lower in TnI-immunized FN14ko ( $n = 15$ ) compared to wt mice ( $n = 12$ ); (inflammation score: FN14ko:  $2.47 \pm 0.31$  vs wt:  $3.58 \pm 0.40$ ;  $P < 0.01$ ; fibrosis score: FN14ko:  $2.07 \pm 0.37$  vs wt:  $3.33 \pm 0.45$ ;  $P < 0.05$ ) (A). Representative macroscopic pictures (column 1) and histopathological examinations (columns 2 and 3) of hearts stained with HE and Afog. Scale bars indicate  $200 \mu\text{m}$  (B). FN14ko mice immunized with TnI ( $n = 14$ ) displayed significantly lower hs-TnT levels compared to wt ( $n = 12$ ) (FN14ko:  $473 \pm 147\text{pg/mL}$  vs wt:  $2586 \pm 823\text{pg/mL}$ ;  $P < 0.01$ ) (C). TnI-immunization led to significantly lower heart weight to body weight ratios in FN14ko mice ( $n = 4$ ) compared to wt ( $n = 4$ ) (FN14ko:  $5.75 \pm 0.67$  vs wt:  $10.38 \pm 1.00$ ;  $P < 0.001$ ) (D). Echocardiographic parameter revealed a better cardiac performance in FN14ko mice immunized with TnI ( $n = 15$ ) compared to wt ( $n = 12$ ); stroke volume (FN14ko:  $18.62 \pm 2.04\mu\text{L}$  vs wt:  $12.00 \pm 1.92\mu\text{L}$ ;  $P < 0.05$ ), left ventricular mass (LV Mass) (FN14ko:  $55.99 \pm 6.49$  mg vs wt:  $81.74 \pm 9.93$  mg;  $P < 0.05$ ), systolic IVS (IVSs), diastolic IVS (IVSd) (IVSs: FN14ko:  $1.54 \pm 0.05$  mm vs wt:  $1.856 \pm 0.11$  mm;  $P < 0.01$ ; IVSd: FN14ko:  $0.85 \pm 0.07$  mm vs wt:  $1.24 \pm 0.14$  mm;  $P < 0.01$ ), LVEF (FN14ko:  $82.4 \pm 2.5\%$  vs wt:  $70.9 \pm 4.4\%$ ;  $P < 0.001$ ) (E). Data are depicted as mean  $\pm$  SEM. Statistical analysis was performed using two-way ANOVA with Bonferroni post hoc test. (For interpretation of the references to color in this figure legend, the reader is referred to the online version of this article.)

Therefore, the impact of the cytokine receptor FN14 on the induction of an EAM was investigated.

For that purpose, it was initially clarified if FN14 plays a role in EAM in general. Here, the results showed that the induction of an EAM led to a significantly increased myocardial FN14 mRNA as well as protein expression level. Similar results could be demonstrated by Mustonen and

colleagues.<sup>23</sup> They observed an increased FN14 mRNA and protein level within 1 day after infarct induction in rats. Moreover, a boost in FN14 expression was detected in a model of Ang II-induced hypertension.<sup>23</sup> These results demonstrate that the expression level of FN14 is upregulated transiently after acute injury and persistently in chronically injured tissue.<sup>7,24</sup> Thus, the upregulation of FN14

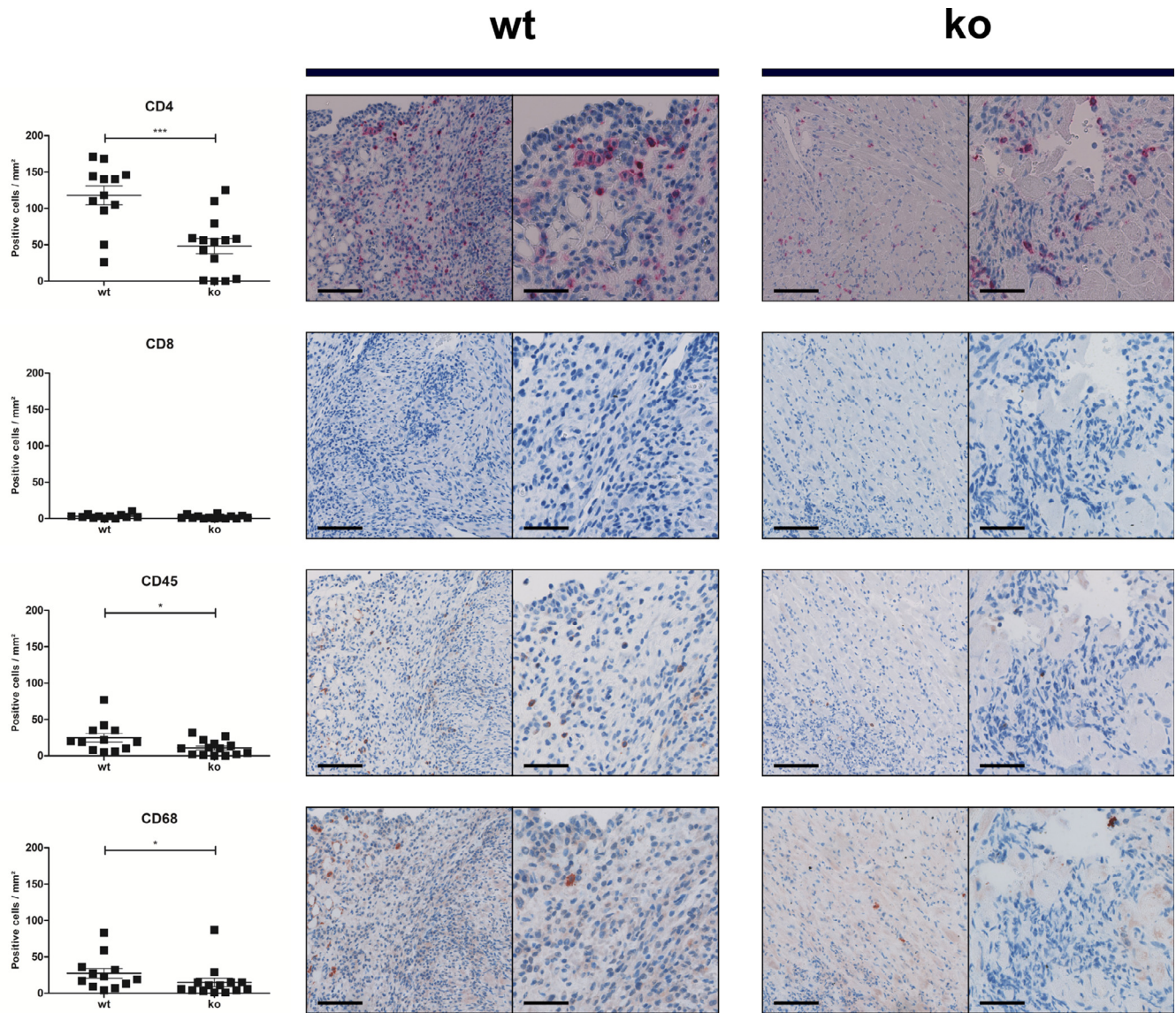


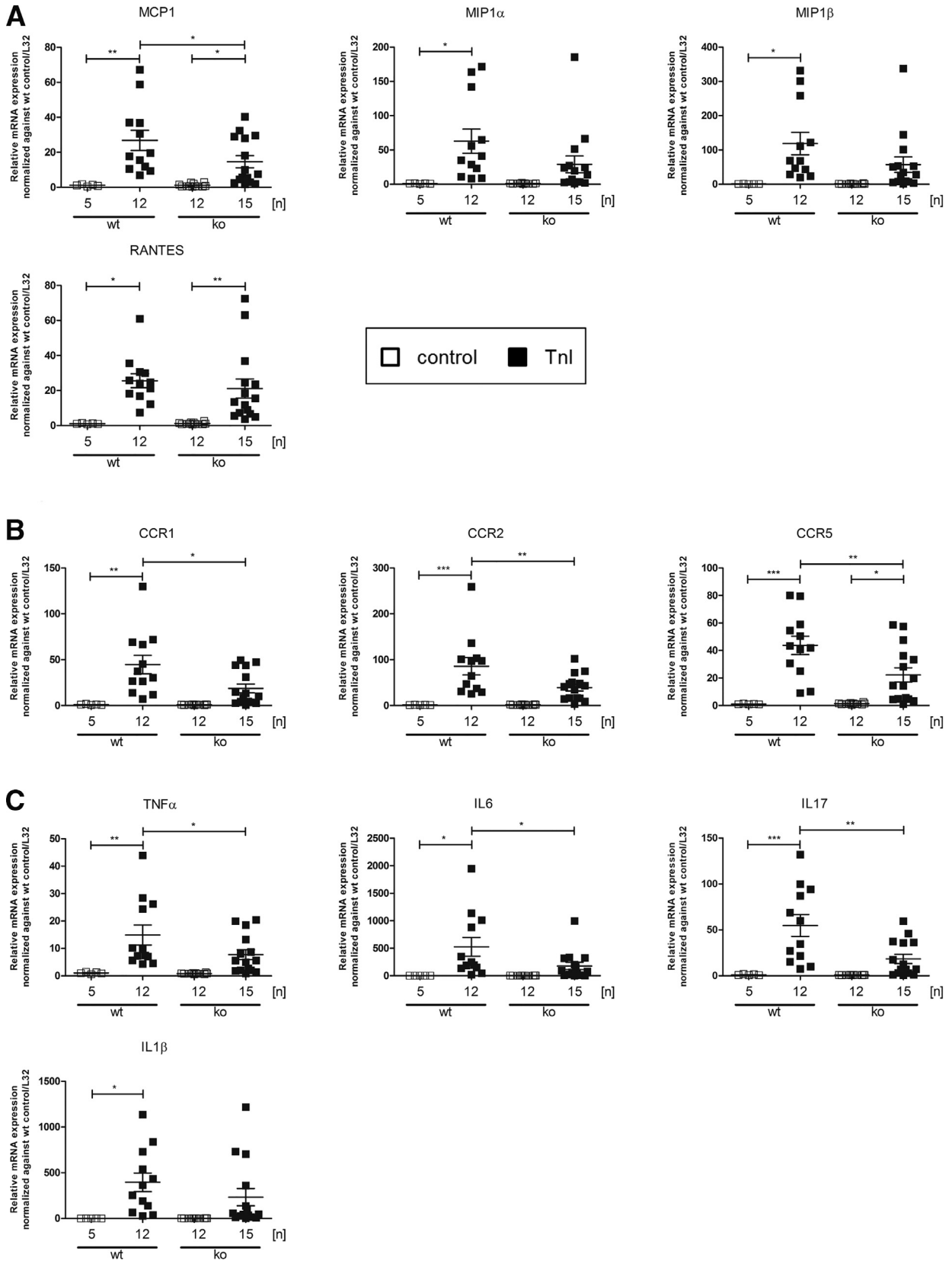
**Fig. 3.** FN14ko mice showed a reduced recruitment of lymphocytes and macrophages in TnI-induced EAM. FN14ko mice and wt littermates were immunized with TnI and sacrificed on day 21. The number of infiltrated CD4 T lymphocytes, B lymphocytes, and macrophages was significantly lower in the hearts of FN14ko (n = 14) compared to wt mice (n = 12) (CD4: FN14ko:  $48.14 \pm 10.56$  vs wt:  $117.9 \pm 12.76$ ;  $P < 0.001$ ; CD45: FN14ko:  $10.86 \pm 2.79$  vs wt:  $24.83 \pm 5.89$ ;  $P < 0.05$ ; CD68: FN14ko:  $14.86 \pm 5.91$  vs wt:  $27.42 \pm 6.68$ ;  $P < 0.05$ ). No difference could be detected for the amount of CD8 T lymphocytes. Scale bars indicate 100  $\mu\text{m}$  (columns 2 and 4) and 50  $\mu\text{m}$  (columns 3 and 5). (For interpretation of the references to color in this figure legend, the reader is referred to the online version of this article.)

seems to be important for the activation of the FN14 signaling in acute injuries.

After these results provided a first clue to a role of FN14 in the pathogenesis of an autoimmune myocarditis, an EAM was induced in mice lacking FN14 to investigate its precise role in disease manifestation. Here, FN14ko mice showed a milder progression of the EAM compared to wt mice. This milder progression found expression in less inflammation and fibrosis as well as better cardiac performance. Furthermore, lower hs-TnT levels could be observed. Usually high hs-TnT levels are associated with the incidence of heart failure and cardiovascular death.<sup>25</sup> Thus, the decreased hs-TnT levels detected in FN14ko mice refers to a cardio protective effect mediated by the inhibition of FN14 signaling. These

results are in accordance with other animal models of inflammatory diseases.<sup>9</sup> In this context, for FN14ko mice a better overall performance could be observed in a lupus as well as a colitis model.<sup>14,15</sup>

In a next step, the effect of FN14 on the recruitment of different leukocyte populations into the myocardium was investigated. With this experiment, it should be ruled out whether the observed milder progression of EAM in FN14ko mice compared to wt mice was triggered by a specific cell type. The results showed that FN14 had an influence on the recruitment of CD4 T lymphocytes, B lymphocytes, and macrophages. In wt mice the amount of these cell types was significantly higher compared to FN14ko mice. In contrast to that, CD8 T lymphocytes do not seem to play an important role in the pathogenesis



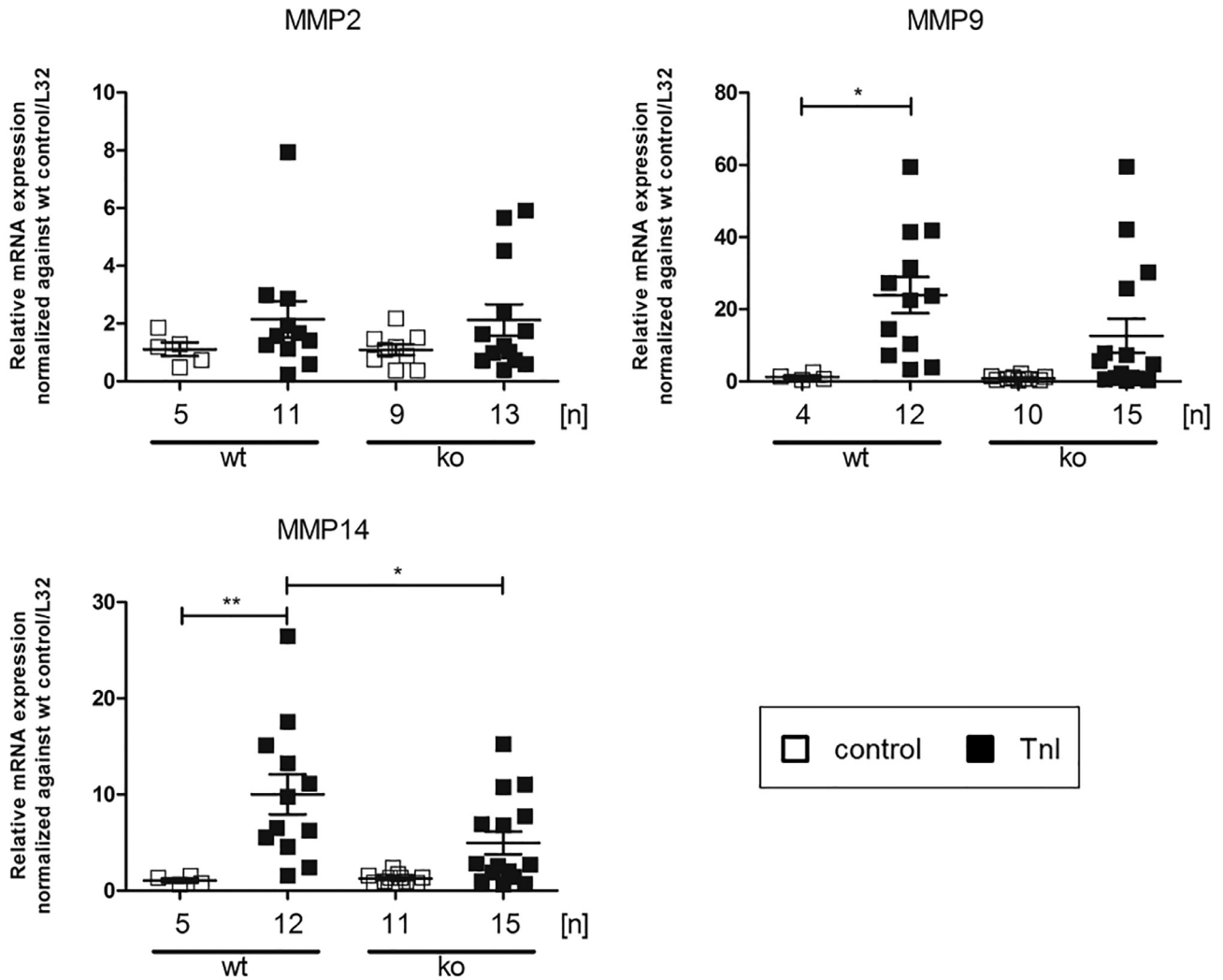


**Fig. 5.** FN14 deficiency affects myocardial mRNA expression of genes involved in cardiac fibrosis. FN14ko mice and wt littermates were immunized with TnI (FN14ko: n = 13–15; wt: n = 11–12) or control (FN14ko: n = 9–11; wt: n = 4–5) and sacrificed on day 21. mRNA expression level of MMP9 was increased in TnI-immunized wt mice compared to mice receiving control (TnI:  $23.93 \pm 5.03$  vs control:  $1.25 \pm 0.46$ ;  $P < .05$ ). MMP14 mRNA expression level was significantly lower in TnI-immunized FN14ko compared to wt mice (FN14ko:  $4.95 \pm 1.18$  vs wt:  $10.01 \pm 2.08$ ;  $P < .05$ ). MMP2 expression did not show any differences between the groups. Data are depicted as means  $\pm$  SEM. Statistical analysis was performed using two-way ANOVA with Bonferroni post hoc test.

of an EAM at all. Thus, only a small amount of CD8 T lymphocytes was recruited to the myocardium in wt as well as FN14ko mice. Nevertheless, the immunohistochemical analysis refers to an impact of FN14 on the innate as well as the

adaptive immune response, which is in line with the findings observed by qPCR experiments.

To better understand the changes in the immune response triggered by FN14ko, the myocardial mRNA expression

**Fig. 4.** Lack of FN14 affects myocardial mRNA expression of genes involved in cardiac inflammation. FN14ko mice and wt littermates were immunized with TnI (FN14ko: n = 15; wt: n = 12) or control (FN14ko: n = 12; wt: n = 5) and sacrificed on day 21. mRNA expression of MCP 1 was significantly lower in TnI-immunized FN14ko compared to wt mice (FN14ko:  $14.63 \pm 3.49$  vs wt:  $26.82 \pm 5.72$ ;  $P < 0.05$ ). mRNA expression of MIP1 $\alpha$  and MIP1 $\beta$  were increased in TnI-immunized wt mice compared to mice receiving control (MIP1 $\alpha$ : TnI:  $62.86 \pm 17.58$  vs control:  $1.15 \pm 0.17$ ;  $P < 0.05$ ; MIP1 $\beta$ : TnI:  $118.7 \pm 32.66$  vs control:  $1.12 \pm 0.16$ ;  $P < 0.05$ ). RANTES was upregulated in both FN14ko and wt mice after TnI-immunization (FN14ko: TnI:  $21.10 \pm 5.44$  vs control:  $1.18 \pm 0.17$ ;  $P < 0.01$ ; wt: TnI:  $25.58 \pm 3.95$  vs control:  $1.05 \pm 0.12$ ;  $P < 0.05$ ). (A) mRNA expression of C–C CCR1, 2, and 5 were significantly lower in TnI-immunized FN14ko compared to wt mice (CCR1: FN14ko:  $18.65 \pm 4.84$  vs wt:  $44.66 \pm 10.08$ ;  $P < 0.05$ ; CCR2: FN14ko:  $39.19 \pm 7.26$  vs wt:  $85.61 \pm 18.97$ ;  $P < 0.01$ ; CCR5: FN14ko:  $22.24 \pm 5.21$  vs wt:  $43.70 \pm 6.66$ ;  $P < 0.01$ ). (B) mRNA levels of cytokines such as TNF $\alpha$ , IL6, and IL17 were significantly decreased in TnI-immunized FN14ko compared to wt mice (TNF $\alpha$ : FN14ko:  $7.72 \pm 1.81$  vs wt:  $14.90 \pm 3.66$ ;  $P < 0.05$ ; IL6: FN14ko:  $176.9 \pm 66.24$  vs wt:  $524.2 \pm 171.0$ ;  $P < 0.05$ ; IL17: FN14ko:  $20.67 \pm 5.49$  vs wt:  $54.75 \pm 11.98$ ;  $P < 0.01$ ). mRNA expression of IL1 $\beta$  was increased in TnI-immunized wt mice compared to mice receiving control (TnI:  $396.3 \pm 102.0$  vs control:  $1.13 \pm 0.31$ ;  $P < 0.05$ ). (C) Data are depicted as means  $\pm$  SEM. Statistical analysis was performed using two-way ANOVA with Bonferroni post hoc test.

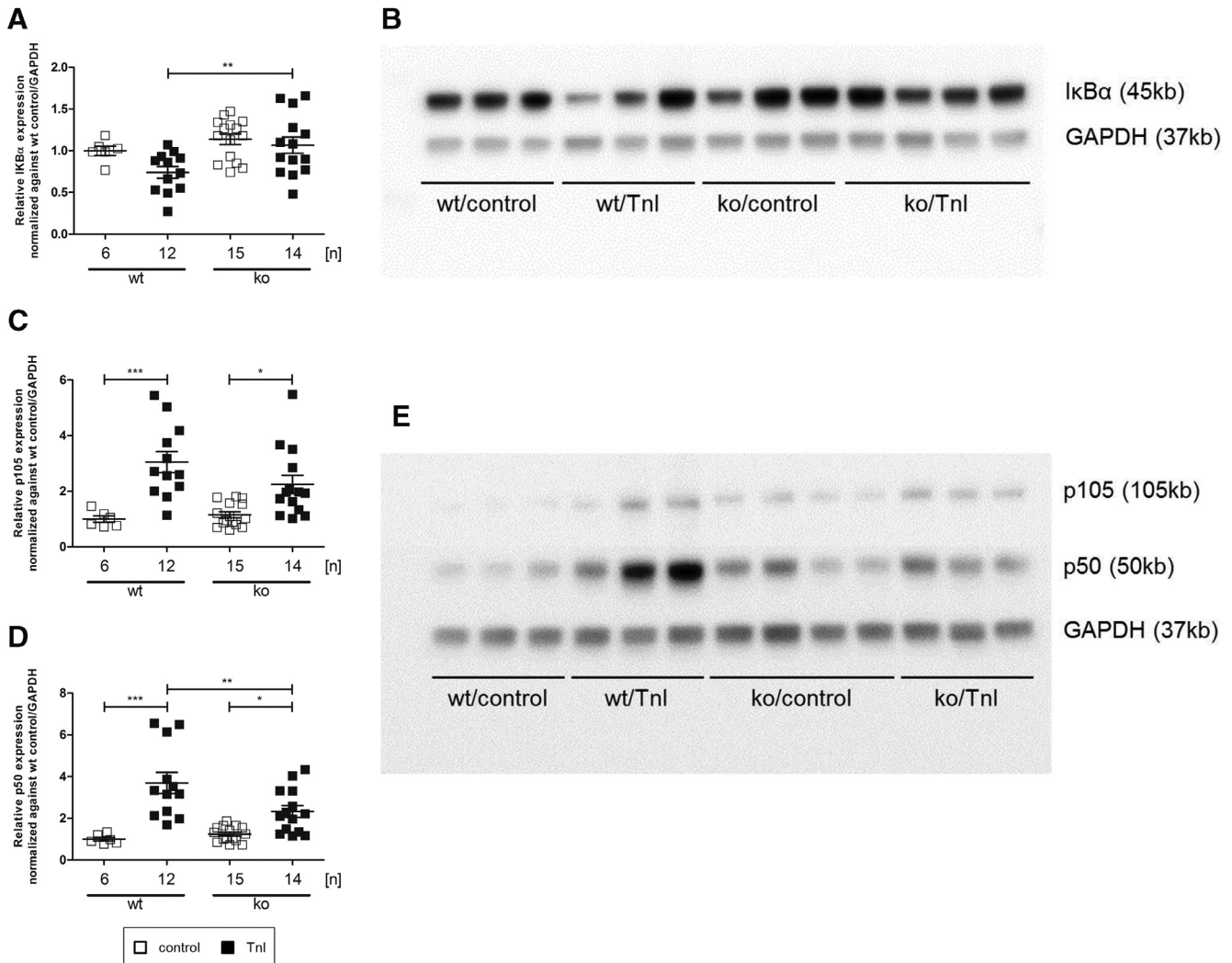


**Fig. 6.** FN14 signaling activated NFκB pathway in TnI-induced EAM. FN14ko mice and wt littermates were immunized with TnI (FN14ko: n = 14; wt: n = 12) or control (FN14ko: n = 15; wt: n = 6) and sacrificed on day 21. Expression of IκBα was decreased in TnI-immunized wt compared to FN14ko-mice (FN14ko:  $1.07 \pm 0.10$  vs wt:  $0.74 \pm 0.07$ ;  $P < 0.01$ ) (A). Representative Western blot images for detection of IκBα protein expression. Ten micrograms of protein were used for detection of IκBα protein expression. GAPDH served as loading control (B). Expression level of p105 was slightly increased in TnI-immunized wt compared to FN14ko-mice (FN14ko:  $2.24 \pm 0.33$  vs wt:  $3.05 \pm 0.38$ ) (C). Expression of p50 was significantly lower in TnI-immunized FN14ko compared to wt mice (FN14ko:  $2.32 \pm 0.28$  vs wt:  $3.70 \pm 0.51$ ;  $P < 0.01$ ) (D). Representative Western blot images for detection of p50 and p105 protein expression. Ten micrograms of protein were used for detection of p50 and p105 protein expression. GAPDH served as loading control (E). Data are depicted as mean  $\pm$  SEM. Statistical analysis was performed using two-way ANOVA with Bonferroni post hoc test. (For interpretation of the references to color in this figure legend, the reader is referred to the online version of this article.)

pattern of various chemokines, their receptors, cytokines, as well as MMPs was determined. In inflammatory processes, chemokines play an important role in the early state because of their chemotactic potential. They are responsible for the directed migration of leukocytes into tissue via their receptors. Because of the diversity in progression of the EAM between FN14ko and wt mice, differences in their chemokine and chemokine receptor expression pattern could be expected. The results of the mRNA analyses showed that the level of the chemokine MCP1 and the levels of the chemokine receptors CCR1, CCR2, and CCR5 are significantly decreased after EAM induction in FN14ko compared to wt mice. Results from former experimental trials support the important role of chemokines in the pathogenesis of heart diseases. Accordingly, Göser

et al<sup>26</sup> were able to show that MCP1 and the receptors CCR2 and CCR5 are crucial in the induction of an EAM. In addition, they described that MCP1 inhibition significantly reduced disease severity. Furthermore, Liehn et al<sup>27</sup> demonstrated that CCR1 contributed to functional impairment and structural remodeling after myocardial infarction (MI). Thus, the improved cardiac parameters in FN14ko mice after EAM induction could be explained by a reduced expression of MCP1 and the chemokine receptors CCR1, CCR2, and CCR5.

After the successful recruitment of leukocytes into cardiac tissue, invaded immune cells produce high amounts of cytokines, which keep pushing the inflammation forward. Thus, pro-inflammatory cytokines like TNFα, IL6, IL1β, and IL17 were upregulated in response to EAM induction in wt mice.

However, the expression of these cytokines was reduced in FN14ko mice after EAM induction indicating that FN14 signaling is essential for their transcription. These results are in accordance with the finding of Park et al,<sup>12</sup> who could describe an enhanced IL17 expression after FN14 stimulation of murine splenocytes. Furthermore, FN14ko mice displayed lower levels of IL6 compared to wt mice in a model of systemic lupus erythematosus.<sup>28</sup> Apart from IL6 and IL17, the FN14 signaling dependent activation of TNF $\alpha$  and IL1 $\beta$  expression, both important cytokines for the induction of an EAM,<sup>29</sup> could be already demonstrated in a colitis and rheumatoid arthritis animal model.<sup>11,30</sup> Thus, it could be assumed that the milder myocardial inflammation observed in FN14ko compared to wt mice is a consequence of lower levels of inflammatory cytokines of mice lacking FN14.

Apart from cytokines, which are essential for the early phase inflammatory processes, MMPs are important factors for the subsequently cardiac remodeling occurring in a later phase of myocarditis. Their involvement in the pathogenesis of cardiomyopathies has been already described.<sup>31–33</sup> MMPs like MMP2, MMP9, and MMP14 can be induced by cytokines like TNF $\alpha$ , IL6, and IL1 $\beta$ .<sup>34,35</sup> Accordingly, in this study it could be observed that the cardiac MMP9 and MMP14 mRNA levels were upregulated during EAM in wt mice, whereas FN14ko mice showed reduced levels of these MMPs. In contrast to that, MMP2 mRNA expression showed no differences depending on the genotype after EAM induction. These differences in the transcriptional expression of MMPs seem to be based on NF $\kappa$ B signaling cascade mediated by FN14.<sup>7,9</sup> This cascade regulates the expression of MMP9 and MMP14, whereas the expression of MMP2 is not effected by NF $\kappa$ B signaling.<sup>36</sup> Thus, the reduced mRNA expression level of MMP9 and MMP14 in FN14ko mice in the EAM model could be ascribed to a decreased activation of NF $\kappa$ B signaling.

To elucidate the impact of FN14ko on NF $\kappa$ B, the expression of NF $\kappa$ B associated proteins was analyzed by Western blot. Here, I $\kappa$ B $\alpha$ , p105, and p50, NF $\kappa$ B signaling molecules, showed different expression levels between wt and FN14ko mice after EAM induction. Accordingly, I $\kappa$ B $\alpha$  protein expression was increased, whereas p50 and p105 protein expression were reduced in FN14ko mice. However, no significant difference could be observed for control-treated wt mice compared to wt mice treated with TnI. This might be ascribed to a type II error because of the small number of animals in the wt control group. Nevertheless, a tendency toward a reduced I $\kappa$ B $\alpha$  protein expression because of EAM induction is detectable in TnI-treated wt mice. FN14ko mice did not show such a decrease in the myocardial I $\kappa$ B $\alpha$  protein amount in response to TnI immunization. Thus, these changes point to a decreased NF $\kappa$ B signaling activation in mice with FN14 depletion. Usually, after FN14 activation I $\kappa$ B $\alpha$ , which inhibits the translocation of NF $\kappa$ B into nucleus, is phosphorylated and subsequently degraded resulting in the release of NF $\kappa$ B. Thus, a higher I $\kappa$ B $\alpha$  level refers to a lower amount of activated NF $\kappa$ B.<sup>37</sup> NF $\kappa$ B itself is a dimer consisting of various subunits including p50, the active derivative of the precursor p105. Accordingly, a decreased expression of the precursor p105

and the dimer subunit p50 observed in FN14o mice, points to a lower amount of activated NF $\kappa$ B as well. Thus, FN14ko not only seems to prevent the translocation of NF $\kappa$ B into the nucleus, but also seems to reduce the NF $\kappa$ B dimer formation leading to a less severe myocarditis. These results are in line with the already demonstrated contribution of NF $\kappa$ B signaling to the pathogenesis of myocarditis, where the severity of EAM could be reduced by inhibition of NF $\kappa$ B activation.<sup>38,39</sup>

Moreover, our findings suggest that the cellular basis for the milder progression of EAM in FN14ko mice could be ascribed to less susceptibility of cardiomyocytes to inflammatory injury. With the exception of primary T and B lymphocytes, FN14 is expressed in almost all cell and tissue types, including cardiomyocytes.<sup>7,8</sup> Under physiological conditions, the FN14 expression is comparably low in cardiomyocytes. However, tissue damage triggered by inflammatory processes can induce an increase in FN14 expression in these cells.<sup>23</sup> Furthermore, it has been previously shown that cardiac fibroblasts as well as cardiomyocytes themselves can secrete proinflammatory cytokines.<sup>40</sup> In addition, a connection between FN14 activation and increased cytokine expression could already be observed in other tissue injury models.<sup>11,28,30</sup> Thus, by an increased FN14 expression, injured cardiac fibroblasts as well as cardiomyocytes seem to maintain an initial myocardial inflammation via activation of downstream signaling cascades resulting in proinflammatory cytokine expression. This FN14 triggered inflammatory response is prevented by the missing FN14 expression in FN14ko mice. Accordingly, the inflammatory response to cardiac injury caused by the experimental autoimmune myocarditis is attenuated in FN14ko mice.

Nevertheless, this study could only give first evidences to an important role of FN14 in the pathogenesis of an inflammatory myocarditis. Although the EAM model is well suited to mimic this human disease in mice, further investigations need to be performed.

## Conclusion

FN14 may play an important role in the pathogenesis of autoimmune myocarditis. Therefore, inhibition of FN14 might represent a novel therapeutic strategy in the treatment of inflammatory cardiomyopathy caused by autoimmune reactions. However, further investigations are necessary to translate these findings in clinical context.

## Disclosures

The authors declare no conflict of interest.

## Acknowledgment

The authors gratefully acknowledge the Center for Model System and Comparative Pathology, Institute of Pathology, University Hospital Heidelberg, Germany and the Tissue Bank of the National Center for Tumor Diseases (NCT) Heidelberg, Germany for immunohistochemical staining and virtual microscopy. We thank Renate Öttl, Stefan Zित्रich and Philipp Hill for excellent technical assistance.

## Supplementary Data

Supplementary data related to this article can be found at doi: [10.1016/j.cardfail.2019.06.003](https://doi.org/10.1016/j.cardfail.2019.06.003).

## References

- Benjamin EJ, Blaha MJ, Chiuve SE, Cushman M, Das SR, Deo R, et al. Heart disease and stroke Statistics-2017 Update: a report from the American Heart Association. *Circulation* 2017;135:e146–603.
- Leuschner F, Katus HA, Kaya Z. Autoimmune myocarditis: past, present and future. *J Autoimmun* 2009;33:282–9.
- Caforio AL, Pankuweit S, Arbustini E, Basso C, Gimeno-Blanes J, Felix SB, et al. Current state of knowledge on aetiology, diagnosis, management, and therapy of myocarditis: a position statement of the European society of cardiology working group on myocardial and pericardial diseases. *Eur Heart J* 2013;34:2636–48. 48a-48d.
- Goser S, Andrassy M, Buss SJ, Leuschner F, Volz CH, Ottl R, et al. Cardiac troponin I but not cardiac troponin T induces severe autoimmune inflammation in the myocardium. *Circulation* 2006;114:1693–702.
- Sanz AB, Sanchez-Nino MD, Ortiz A. TWEAK, a multifunctional cytokine in kidney injury. *Kidney Int* 2011;80:708–18.
- Ortiz A, Sanz AB, Munoz Garcia B, Moreno JA, Sanchez Nino MD, Martin-Ventura JL, et al. Considering TWEAK as a target for therapy in renal and vascular injury. *Cytokine Growth Factor Rev* 2009;20:251–8.
- Winkles JA. The TWEAK-Fn14 cytokine-receptor axis: discovery, biology and therapeutic targeting. *Nat Rev Drug Discov* 2008;7:411–25.
- Chorianopoulos E, Heger T, Lutz M, Frank D, Bea F, Katus HA, et al. FGF-inducible 14-kDa protein (Fn14) is regulated via the RhoA/ROCK kinase pathway in cardiomyocytes and mediates nuclear factor-kappaB activation by TWEAK. *Basic Res Cardiol* 2010;105:301–13.
- Xu WD, Zhao Y, Liu Y. Role of the TWEAK/Fn14 pathway in autoimmune diseases. *Immunol Res* 2016;64:44–50.
- Lu J, Kwan BC, Lai FM, Choi PC, Tam LS, Li EK, et al. Gene expression of TWEAK/Fn14 and IP-10/CXCR3 in glomerulus and tubulointerstitium of patients with lupus nephritis. *Nephrology (Carlton)* 2011;16:426–32.
- Park JS, Kwok SK, Lim MA, Oh HJ, Kim EK, Jhun JY, et al. TWEAK promotes osteoclastogenesis in rheumatoid arthritis. *Am J Pathol* 2013;183:857–67.
- Park JS, Park MK, Lee SY, Oh HJ, Lim MA, Cho WT, et al. TWEAK promotes the production of Interleukin-17 in rheumatoid arthritis. *Cytokine* 2012;60:143–9.
- Park MC, Chung SJ, Park YB, Lee SK. Relationship of serum TWEAK level to cytokine level, disease activity, and response to anti-TNF treatment in patients with rheumatoid arthritis. *Scand J Rheumatol* 2008;37:173–8.
- Xia Y, Herlitz LC, Gindea S, Wen J, Pawar RD, Misharin A, et al. Deficiency of fibroblast growth factor-inducible 14 (Fn14) preserves the filtration barrier and ameliorates lupus nephritis. *J Am Soc Nephrol* 2015;26:1053–70.
- Son A, Oshio T, Kawamura YI, Hagiwara T, Yamazaki M, Inagaki-Ohara K, et al. TWEAK/Fn14 pathway promotes a T helper 2-type chronic colitis with fibrosis in mice. *Mucosal Immunol* 2013;6:1131–42.
- Jain M, Jakubowski A, Cui L, Shi J, Su L, Bauer M, et al. A novel role for tumor necrosis factor-like weak inducer of apoptosis (TWEAK) in the development of cardiac dysfunction and failure. *Circulation* 2009;119:2058–68.
- Shi J, Jiang B, Qiu Y, Guan J, Jain M, Cao X, et al. PGC1 $\alpha$  plays a critical role in TWEAK-induced cardiac dysfunction. *PLoS One* 2013;8:e54054.
- Jarr KU, Eschricht S, Burkly LC, Preusch M, Katus HA, Frey N, et al. TNF-like weak inducer of apoptosis aggravates left ventricular dysfunction after myocardial infarction in mice. *Mediators Inflamm* 2014;2014:131950.
- Jakubowski A, Ambrose C, Parr M, Lincecum JM, Wang MZ, Zheng TS, et al. TWEAK induces liver progenitor cell proliferation. *J Clin Invest* 2005;115:2330–40.
- Andrassy M, Volz HC, Schuessler A, Gitsioudis G, Hofmann N, Laohachewin D, et al. HMGB1 is associated with atherosclerotic plaque composition and burden in patients with stable coronary artery disease. *PLoS One* 2012;7:e52081.
- Krejci J, Mlejnek D, Sochorova D, Nemecek P. Inflammatory Cardiomyopathy: a current view on the Pathophysiology, Diagnosis, and treatment. *Biomed Res Int* 2016;2016:4087632.
- Weintraub RG, Semsarian C, Macdonald P. Dilated cardiomyopathy. *Lancet* 2017;390:400–14.
- Mustonen E, Sakkinen H, Tokola H, Isopoussu E, Aro J, Leskinen H, et al. Tumour necrosis factor-like weak inducer of apoptosis (TWEAK) and its receptor Fn14 during cardiac remodelling in rats. *Acta Physiol (Oxf)* 2010;199:11–22.
- Burkly LC. TWEAK/Fn14 axis: the current paradigm of tissue injury-inducible function in the midst of complexities. *Semin Immunol* 2014;26:229–36.
- Omland T, de Lemos JA, Sabatine MS, Christophi CA, Rice MM, Jablonski KA, et al. A sensitive cardiac troponin T assay in stable coronary artery disease. *N Engl J Med* 2009;361:2538–47.
- Göser S, Ottl R, Brodner A, Dengler TJ, Torzewski J, Ega-shira K, et al. Critical role for monocyte chemoattractant protein-1 and macrophage inflammatory protein-1 $\alpha$  in induction of experimental autoimmune myocarditis and effective anti-monocyte chemoattractant protein-1 gene therapy. *Circulation* 2005;112:3400–7.
- Liehn EA, Merx MW, Postea O, Becher S, Djalali-Talab Y, Shagdarsuren E, et al. Ccr1 deficiency reduces inflammatory remodelling and preserves left ventricular function after myocardial infarction. *J Cell Mol Med* 2008;12:496–506.
- Zhao Z, Burkly LC, Campbell S, Schwartz N, Molano A, Choudhury A, et al. TWEAK/Fn14 interactions are instrumental in the pathogenesis of nephritis in the chronic graft-versus-host model of systemic lupus erythematosus. *J Immunol* 2007;179:7949–58.
- Rose NR. Critical cytokine pathways to cardiac inflammation. *J Interferon Cytokine Res* 2011;31:705–10.
- Kawashima R, Kawamura YI, Oshio T, Son A, Yamazaki M, Hagiwara T, et al. Interleukin-13 damages intestinal mucosa via TWEAK and Fn14 in mice—a pathway associated with ulcerative colitis. *Gastroenterology* 2011;141:2119–29. e8.
- Spinale FG. Myocardial matrix remodeling and the matrix metalloproteinases: influence on cardiac form and function. *Physiol Rev* 2007;87:1285–342.
- Spinale FG, Coker ML, Heung LJ, Bond BR, Gunasinghe HR, Etoh T, et al. A matrix metalloproteinase induction/activation system exists in the human left ventricular myocardium and is upregulated in heart failure. *Circulation* 2000;102:1944–9.
- Tsoutsman T, Wang X, Garchow K, Riser B, Twigg S, Semsarian C. CCN2 plays a key role in extracellular matrix gene

- expression in severe hypertrophic cardiomyopathy and heart failure. *J Mol Cell Cardiol* 2013;62:164–78.
34. Liu P, Sun M, Sader S. Matrix metalloproteinases in cardiovascular disease. *Can J Cardiol* 2006;22(Suppl B):25B–30B.
  35. Briasoulis A, Tousoulis D, Papageorgiou N, Kampoli AM, Androulakis E, Antoniadis C, et al. Novel therapeutic approaches targeting matrix metalloproteinases in cardiovascular disease. *Curr Top Med Chem* 2012;12:1214–21.
  36. Fanjul-Fernandez M, Folgueras AR, Cabrera S, Lopez-Otin C. Matrix metalloproteinases: evolution, gene regulation and functional analysis in mouse models. *Biochim Biophys Acta* 2010;1803:3–19.
  37. Yamamoto Y, Gaynor RB. I $\kappa$ B kinases: key regulators of the NF- $\kappa$ B pathway. *Trends Biochem Sci* 2004;29:72–9.
  38. Valaperti A. Drugs targeting the canonical NF- $\kappa$ B pathway to treat viral and autoimmune myocarditis. *Curr Pharm Des* 2016;22:440–9.
  39. Watanabe R, Azuma RW, Suzuki J, Ogawa M, Itai A, Hirata Y, et al. Inhibition of NF- $\kappa$ B activation by a novel IKK inhibitor reduces the severity of experimental autoimmune myocarditis via suppression of T-cell activation. *Am J Physiol Heart Circ Physiol* 2013;305:H1761–71.
  40. Aoyagi T, Matsui T. The cardiomyocyte as a source of cytokines in cardiac injury. *J Cell Sci Ther* 2011;2012:003.